Research on Chemical Intermediates (2018) 44:6549–6567
https://doi.org/10.1007/s11164-018-3508-8

Textural, structural and catalytic behavior of low specific area silica-supported copper catalysts: effect of preparation method

Ibtissem Lounas[1] · Hanane Zazoua[1,2] · Adel Saadi[1] · Zahia Mesbah Benyoucef[3]

Received: 2 March 2018 / Accepted: 12 June 2018 / Published online: 18 June 2018

Abstract

Supported copper catalysts on low surface area silica were prepared by several methods and characterized by AAS, XRD, N_2 adsorption, SEM, H_2-TPR, N_2O titration, TGA-DTA, UV–Vis techniques. Their hydrogenating properties were examined in the gas-phase hydrogenation of benzaldehyde. The analysis of characterization results revealed that the choice of preparation method affected the texture, composition, and structure of the calcined and reduced Cu/SiO_2 catalysts. The dispersion and size distribution of copper species was present in different forms in the catalysts that exhibited low specific surface areas. In gas-phase hydrogenation of benzaldehyde to benzyl alcohol, the catalysts tested at the reaction temperatures of 160 and 200 °C were stable and conducted to a good catalytic activity and benzyl alcohol selectivity ranging between 5 and 39 μmol min^{-1} g^{-1} and 0–95%, respectively. The activity of the catalysts in gas-phase hydrogenation also depended on the particle size and the nature of copper species formed on low surface area silica.

Keywords Cu/SiO_2 · Benzaldehyde · Benzyl alcohol · Hydrogenation · Hydrogenolysis

✉ Adel Saadi
asaadi@usthb.dz

[1] Laboratory of Natural Gas Chemistry, Faculty of Chemistry, USTHB University, PO Box 32, 16111 El-Alia, Bab-ezzouar, Algiers, Algeria

[2] Research Center in Analytical Chemistry and Physics (CRAPC), PO Box 248, Bou-Ismail, Tipaza, Algeria

[3] Department of Chemistry, Montmorency College, 475 Boulevard de l'Avenir, Laval, QC H7N 5H9, Canada

Introduction

Benzyl alcohol is an important product used in the chemical industry, notably in fine chemicals. It is found in several fields, such as cosmetics, as a solvent and preservative [1], but also in the food and pharmaceutical industries [2]. In industry, benzyl alcohol is obtained by refluxing benzyl chloride, a long and, therefore, costly process, which yields benzyl ether in large quantities [3] or by chlorination of toluene followed by hydrolysis, except that this process is very toxic to the environment [4]. For this reason, many researchers are interested in a cheaper and especially cleaner way of producing benzyl alcohol using homogeneous or heterogeneous catalysts. Conscious of the difficulties to use homogeneous catalysts, especially in the catalyst–product separation, heterogeneous catalysts have been investigated in the hydrogenation of benzaldehyde. This reaction has been the subject of many works because of its simplicity to be implemented and which help us to understand the mechanism of the latter [5]. In the last few years, considerable works have been devoted to the reduction of benzaldehyde over supported precious metal catalysts [6, 7], supported noble metal catalysts [8–10] or metal oxide catalysts [11, 12], in liquid or gaseous phases [13, 14]. Recently, Nagaraja et al. [15] published a review article describing the successful use of several catalysts for catalytic hydrogenation of benzaldehyde for the selective synthesis of benzyl alcohol. Various factors may be involved in the reduction of benzaldehyde and favor benzyl alcohol formation, such as active metals [16, 17], acidic or basic properties of support [18], effect of interaction oxygen support-hydrogen flow [19], effect of electronic and geometric properties of the active phase influenced by the support and catalysts preparation method [20–22]. Depending on the catalyst and operating conditions, benzaldehyde can be reduced to toluene with benzyl alcohol as intermediate or to benzene as end-product of hydrogenation or hydrogenolysis reaction, respectively [23].

In the literature, it has been shown that copper-based materials appear as excellent catalysts because of their high activity for vapor-phase hydrogenation reactions [24–27], it has been suggested that metallic copper sites are active for the selective hydrogenation of C − O bonds and are relatively inactive for the hydrogenolysis of C − C bonds [28]. Our previous work and the literature on Cu catalysts supported on silica indicated that high dispersion of copper species and strong metal−support interactions are important factors to explain the high activity and stability in hydrogenation of benzaldehyde [15]. In addition, the copper is never used as a bulk catalyst it always comes with an additive and/or in the supported form in order to have a better dispersion of the copper species [29]. Furthermore the higher activity of Cu/SiO_2 compared to other catalysts is related to the better reducibility of the copper due to the large surface area and to the participation of acid–base properties of the silica support. Under hydrogen atmosphere a high benzaldehyde conversion and benzyl alcohol selectivity are obtained only with copper supported over acidic silica, which prevents adsorption of benzyl alcohol formed during the hydrogenation of benzaldehyde. The mechanism may be due to active hydrogen species at the surface of catalysts generated by homolytic or

heterolytic cleavage of hydrogen molecule, which directly reacts with benzaldehyde to give toluene and benzyl alcohol [30].

The high activity of a copper-based supported catalyst often requires a highly active surface area and, therefore, for small particles, i.e., a high dispersion of the active phase; because small metal particles can sinter even at relatively low temperatures, these generally are used in a support material, which itself is thermally stable [31]. With an inert support such as silica, other important physical characteristics such as texture (specific surface area, pore size distribution, and porous volume), density, and mechanical strength can be established [32]. Munnik et al. [33] recently published a review that summarizes the influence of catalysts preparation method, beyond the nature of the metal and its charge. In fact, they highlight that the effect of conventional and unconventional methods of preparation could have a direct influence on the dispersion of a metal on the support, and consequently on the catalytic properties of the materials. However, some methods of preparation often make it difficult to control the morphology of the final material [34, 35], hence the need to search for new alternative methods capable of obtaining supported catalysts with well-defined metal particles is the preparation of supported catalysts [36].

Amorphous silica is usually used as a support because of its important physical properties, thermally stable and maintains a high specific surface area up to high temperatures, it is also known that it does not promote the formation of mixed oxides and it provides a better approach of the particle size effect on the behavior of supported catalysts. In addition, copper-based catalysts have generally been supported using high surface area materials and higher than 5 wt%. In our work, we have found it also interesting to study the crystalline silica material with low surface area as a support for a low copper weight because no studies have been done and also to give rise to an important contribution to the corpus of literature.

The present study reports the results obtained over 3.0 wt% of copper supported on crystalline silica of low area prepared by several methods. The stability and surface properties of the copper particles were examined by different characterization techniques and correlated to their catalytic activity in benzaldehyde hydrogenation.

Experimental

Catalysts preparation

The Cu/SiO_2 samples were prepared from SiO_2 Aldrich® and $Cu(NO_3)_2{\cdot}3H_2O$ (Panreac 99%) precursors with a content of 3.0 wt% by several methods:

1. Deposition–precipitation (DP) synthesis: catalyst DP is prepared by precipitating a solution of copper nitrate (0.5 M) by sodium carbonate at pH $\sim$ 7 in temperature average of 85–90 °C in the presence of SiO_2 support. After precipitation, the solid is washed and dried at 100 °C overnight.
2. Ionic-exchange (IE) method: catalyst IE is obtained by ionic exchange. An aqueous solution of copper nitrate (0.5 M) is brought to a pH $\sim$ 13 by the

addition of concentrated ammonia. The SiO_2 support is previously added to an ammonia solution at the same pH and stirred for 6 h at room temperature. Then the $[Cu(NH3)_4]^{2+}$ complex is added and the mixture is stirred and evaporated. The solid is washed with an ammonia solution and dried overnight at 100 °C.

3. Sol–gel (SG) method: the catalyst SG is prepared by sol–gel method from SiO_2 as support mixed with ethanol and an aqueous solution of copper nitrate (0.5 M). The molar ratio $SiO_2/C_2H_5OH/H_2O$ (1/6/8) is added to tetra-ammonia as complex agent. The mixture is placed under stirring and the obtained gel is dried at 100 °C overnight.
4. Hydrolysis (HY) method: the catalyst HY is prepared first of all by adding an aqueous copper nitrate solution (0.5 M) to a concentrated ammonia 25 wt%; this solution mix is placed under stirring at a pH equal to 9 instead to form the $[Cu(NH_3)_4]^{2+}$ complex. Then the SiO_2 support is added to the mixture and stirred for 30 min; the dough obtained is then placed in an ice bath at 0 °C, and 500 mL of distilled water is added dropwise to the suspension to hydrolyze the copper complex. Finally, the solution is filtered, washed three times and dried at 100 °C overnight.

After the drying step, all samples are calcined in air flow at 350 °C for 3 h with a heating rate of 5 °C/min, characterized by different methods and tested in the hydrogenation reaction.

Characterization techniques

The contents of copper were determined by atomic absorption spectroscopy (AAS) using a Perkin Elmer Analyst 700 apparatus. The samples were dissolved in a 3:1 mixture of HCl/HNO_3 solution. Powder X-ray diffraction (XRD) patterns were recorded on a Philips X'pert Pro diffractiometer with Cu-K_α radiation (λ = 0.154 nm). Diffractograms were collected at room temperature from 10° to 80° range with a scanning step size of 0.02° and a counting time of 1 s.

Nitrogen-physisorption measurements were performed at − 196 °C using an ASAP 2020 Micromeritics instrument. Before each measurement the samples were first outgassed at 700 °C for 12 h and then at room temperature for 2 h. The BET method was used to determine the specific surface areas whereas pore volumes/diameters were calculated by the BJH theory [37].

H_2-Temperature-programmed reduction (H_2-TPR) of samples were carried out on a Micromeritics II-Autochem 2920 instrument, using H_2/Ar (5% v/v) as the reducing gas mixture. The sample of 100 mg mass was heated from room temperature to 850 °C at a heating rate of 7 °C/min after pretreatment at 350 °C in argon gas flow. The H_2 (total flow 25 mL/min) consumed during the experiment was measured with a thermal conductivity detector (TCD). The water formed during the reduction of the catalyst was condensed and trapped by a cold mixture (isoprapanol + liquid nitrogen, T = − 60 °C) and copper loading was estimated from the H_2 consumption by assuming the following reduction stoechiometry: $CuO + H_2 \rightarrow Cu + H_2O$. The copper surface areas and copper dispersions were determined according to N_2O titration using the same equipment. Before

measurements the calcined sample underwent a H_2-TPR process in H_2/Ar (5% v/v) as reducing gas mixture from 50 to 500 °C for 2 h. After cooling down, the sample was exposed to N_2O/Ar (5% v/v) and oxidized at a flow rate of 25 ml/min at 60 °C for 1 h, followed by Ar purging and cooling the sample bed down to room temperature. Finally, H_2-TPR was passed again with a gas mixture of H_2/Ar to 500 °C. Copper dispersion was calculated by dividing the amount of surface copper sites by the total number of Cu atoms; copper surface area was calculated by assuming spherical shape of the Cu metal particles and a surface concentration of 1.47×10^{19} Cu atoms/m^2.

Thermal gravimetry analysis (TGA) was performed by an SDT Q600 TA Instruments heating rate 10 °C/min (nitrogen flow of 100 mL/min) and the materials were placed in an alumina crucible. Diffuse reflectance UV–Vis spectroscopic measurements were performed by SPECORD Plus spectrometer. The spectra were collected at 200–1100 nm referenced to $BaSO_4$. The scanning electronic microscopy (SEM) images were acquired with a Fei-Quanta 250 microscope.

Catalytic experiments

The catalytic performances of the samples were evaluated in the gas phase hydrogenation of benzaldehyde at reaction temperatures of 160 and 200 °C using a fixed-bed glass tubular reactor with 200 mg samples at atmospheric pressure and a total flow rate of 50 cm^3 min^{-1}. Before the catalytic test, each catalyst was reduced in situ for 2 h at 250 °C in a current of H_2 with a flow rate of 20 cm^3 min^{-1}. Gaseous benzaldehyde was obtained by bubbling of nitrogen gas in liquid benzaldehyde (Aldrich, 99.98%) maintained at constant temperature (50 °C) in a suitable saturator. After the pre-reduction step, the reactant gas feed consisted of 4.8 torr of benzaldehyde and 250 torr of H_2 diluted in N_2 (total flow rate of 50 cm^3 min^{-1}).

The gaseous reactant and products were analyzed on line using a Delsi IGC-121 ML chromatograph equipped with a FID detector and 10% CP-SIL 8 CB/Chromosorb W column. Each reaction temperature was maintained constant until the corresponding steady-state was reached as indicated by the gas chromatograph analysis of the exit gases samples. Finally, no mass transfer was observed with 200 mg of the sample weight.

Results and discussion

Catalysts characterization

Copper loading and BET surface data of SiO_2, DP, EI, SG and HY catalysts are summarized in Table 1.

The elemental composition of catalysts was determined by atomic absorption spectroscopy, and the results show that the samples contain only the copper phase on silica support. The Cu contents are very close to the nominal value of 3% weight

Table 1 Textural and structural properties of SiO_2 and Cu/SiO_2 catalysts

Catalyst	SiO_2	Cu/SiO_2-DP	Cu/SiO_2-IE	Cu/SiO_2-SG	Cu/SiO_2-HY
Cu loading (wt%)[a]	–	3.1	2.3	3.2	3.3
S_{BET} ($m^2\ g^{-1}$)	7.0	8.4	8.3	8.3	9.1
Average pore volume ($cm^3\ g^{-1}$)[b]	0.0035	0.0079	0.0080	0.0192	0.0228
Average pore diameter (nm)[b]	36.0	5.2	5.4	13.0	15.4
Theoretical H_2 consumption (mmol)[c]	–	48.8	36.2	50.4	51.9
Experimental H_2 consumption (mmol)[c]	–	45.6	34.5	46.8	44.6
% of total H_2 consumption[c]	–	93.4	95.3	92.9	85.9
Cu^0 surface area ($m^2\ g^{-1}$)[d]	–	1.3	3.1	2.4	3.5
Copper dispersion degree (%)	–	38.4	29.3	30.9	25.5

[a]Determined by AAS method

[b]Determined using BJH method

[c]Calculated assuming total reduction of Cu/SiO_2

[d]Determined by N_2O titration

except on Cu/SiO_2-IE catalysts, which exhibit a Cu content at around about 2.3 wt%, indicating an incomplete exchange with the Cu species.

The decomposition of Cu/SiO_2 precursors was studied by TGA technique under nitrogen flow in the temperature range 50–650 °C (Fig. 1). The obtained curves show essentially three main and well-defined mass losses: (1) the first step appearing below 200 °C is attributed to the desorption of physisorbed water [38], (2) the second step situated between 200 and 350 °C corresponded to the decomposition of nitrate and ammonium ions giving CuO phase [39], (3) the last step appearing above 350 °C is probably due to the decomposition of carbonate species and copper complex [40]. The analyzed results show that setting the calcination temperature at 350 °C does not make it possible to eliminate all the impurities that resisted washing during the preparation except for the "SG" and "IE" precursors.

The successive weight losses (%), the corresponding temperatures and the nature of evolved gases observed in the TGA curves show that the decomposition of "IE" and "SG" precursors conducted to two mass losses, whereas "HY" and "DP" precursors show three mass losses. The first weight loss common to all precursors at 100 °C to ca. 200 °C can be attributed to the corresponding to the removal of physisorbed water with a mass loss of 0.8–4.5%. The second decomposition step, which starts at 200 °C and ends at 450 °C, may be caused by the departure of nitrate and ammonium ions (weight loss: 1.1–18%). A continuous weight loss occurs above 450 °C, appears only on "HY" and "DP" precursors and is attributed to the decomposition of carbonate and complex $[Cu(NH_3)_4]^{2+}$ species.

Figure 2 shows the XRD patterns of SiO_2 (a), Cu/SiO_2-IE (b), Cu/SiO_2-SG (c), Cu/SiO_2-HY (d), Cu/SiO_2-DP (e) catalysts calcined at 350 °C, and the results only

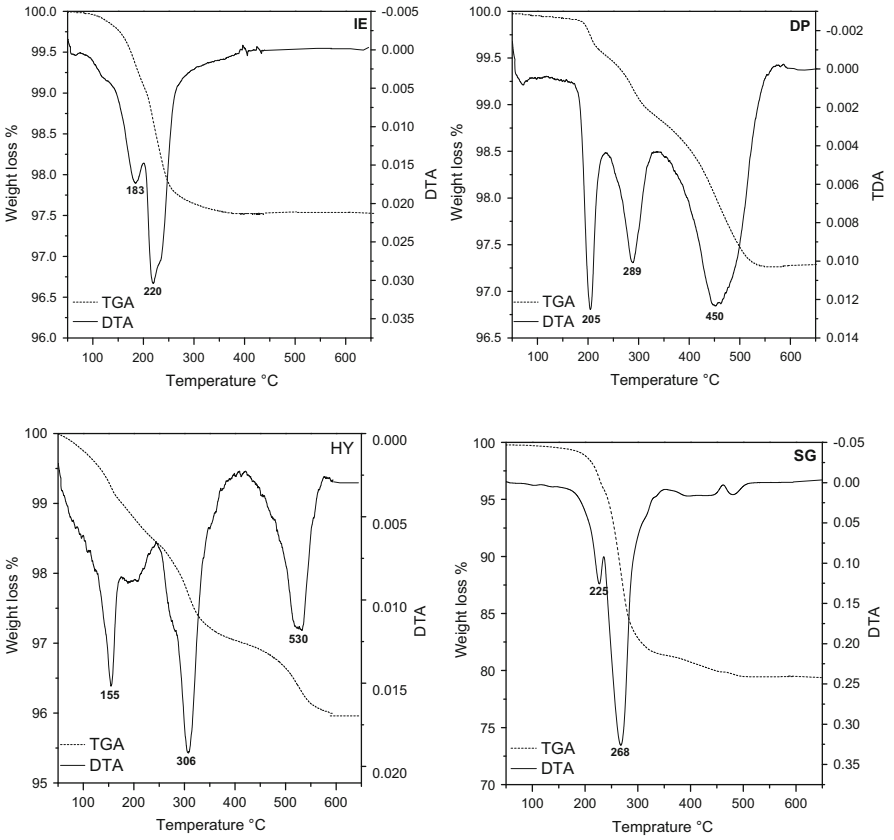

Fig. 1 TGA-DTA curves of Cu/SiO_2-IE, Cu/SiO_2-DP, Cu/SiO_2-HY, Cu/SiO_2-SG. Measurements done under nitrogen flow 100 mL/min, from 50 to 650 °C with 10 °C/min rate

exhibit the characteristic diffractions of a highly crystalline SiO_2-like phase (Fig. 2a). The wide angle powder XRD of calcined CuO/SiO_2 catalysts display typical images of quartz SiO_2 species positioned at 21°, 26°, 50° corresponding to (100), (101) and (112) lattice planes (JCPDS-ICDD card: 46-1045). However, no reflection plan due to crystalline copper species (CuO, JCPDS-ICDD card: 05-0661) and (Cu_2O, JCPDS-ICDD card: 05-0667), copper hydroxide ($Cu(OH)_2$, JCPDS-ICDD card: 35-0505), or either metallic copper (JCPDS-ICDD card: 04-0836) appear for any of the catalysts, which can be explained by the presence of amorphous or very small copper species highly dispersed within the matrix [41, 42].

The textural properties and the N_2 adsorption isotherms of calcined Cu/SiO_2 catalysts are given in Table 1 and Fig. 3. The results show that SiO_2 support and Cu/SiO_2 catalysts exhibit low and similar specific surface area with a value does not exceed 10 $m^2\ g^{-1}$. The BET surface area of the catalysts increases weakly compared to the surface of the silica support and this increase is the same order for each catalyst independently of the preparation method. The gap of the specific

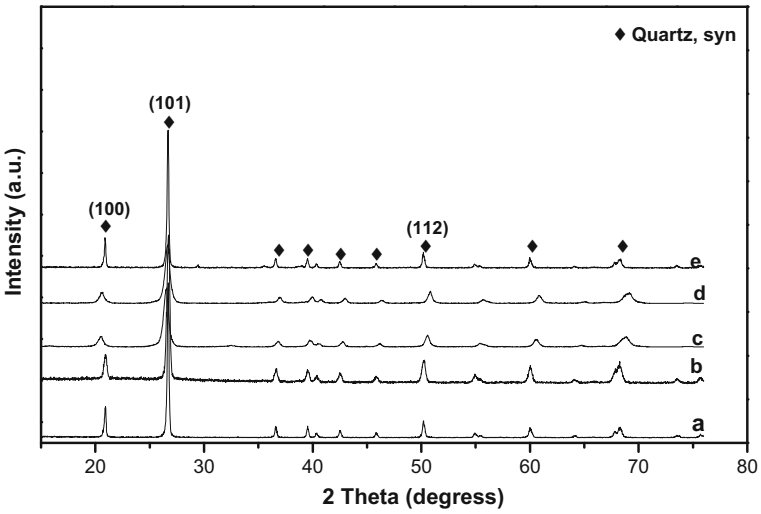

Fig. 2 X-ray diffraction patterns of calcined: a SiO_2, b Cu/SiO_2-IE, c Cu/SiO_2-SG, d Cu/SiO_2-HY, e Cu/SiO_2-DP catalysts. Filled diamond SiO_2, Quartz. Scanning step of 0.02° under Cu-Kα radiation ($\lambda = 0.154$ nm)

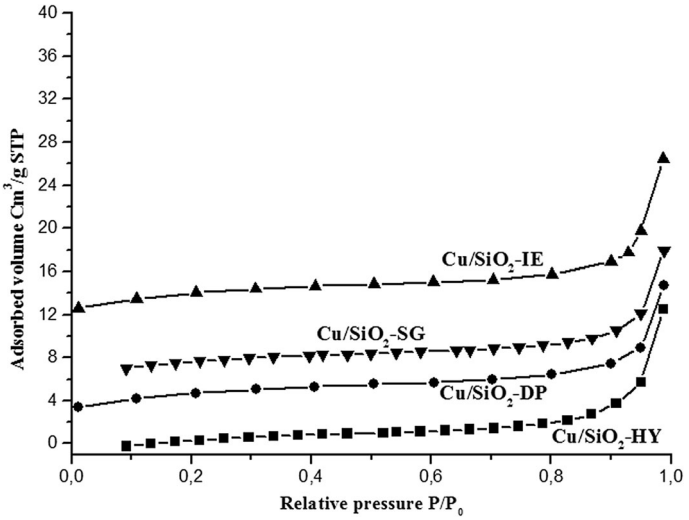

Fig. 3 Nitrogen adsorption isotherms of samples prepared by several methods

surface area (20–30%) can be attributed to the addition of copper and calcination effect.

According to IUPAC classification of adsorption isotherms, Fig. 3 shows that the isotherms are typical of type II and the mean pore diameters calculated by BJH theory indicate that all catalysts are in the mesoporous range (Table 1), but probably contain also some macropores and/or non-porous grain aggregates. The comparison

of mean pore volume and diameter reveals that "DP" and "IE" catalysts are similar with a pore volume (pore diameter) of around 0.008 $cm^3\ g^{-1}$ (5.3–5.4 nm). The same result is obtained for "SG" and "HY" catalysts with pore volume (pore diameter) of around 0.02 $cm^3\ g^{-1}$ (13–15.4 nm). The decrease of mean pore volume and diameter on "DP" and "IE" catalysts can be related to the placement of copper nanoparticles around and inside the pores.

The H_2-TPR measurement was carried out to study the redox properties of samples previously calcined at 350 °C and the interaction between the copper species and the low surface area silica support. It is especially suitable for studying highly dispersed systems with low loading [43]. The obtained profiles of reduced copper supported catalysts are represented in Fig. 4, and the reduction of copper species is accomplished at different temperatures, which starts at 230 °C and ends at 450 °C. Despite the low copper content (3% wt) on silica support, the TPR profiles show that each catalyst has a particular profile; therefore, it can be assumed that each method of preparation provides different characteristics to each catalyst. Indeed, the catalyst prepared by hydrolysis "HY" was reduced in one single step (258 °C), the "DP" catalyst in two steps (396–412 °C), the "IE" catalyst in three steps (238–305–356 °C) and finally the "SG" catalyst in four steps (292–350–362–414 °C). The appearance of several reduction peaks indicates the presence of copper nanoparticles with of different sizes in more or less strong interaction with silica support. It is well known that CuO phase can be reduced in the temperature range 230–500 °C [43] and may be related to the copper content, method of preparation and the nature of the support.

The TPR study made by Dow et al. [44, 45] showed that two peaks were obtained. The first peak appearing in the low temperature region is attributed to the reduction of a highly dispersed copper species, including isolated Cu^{2+} ions that

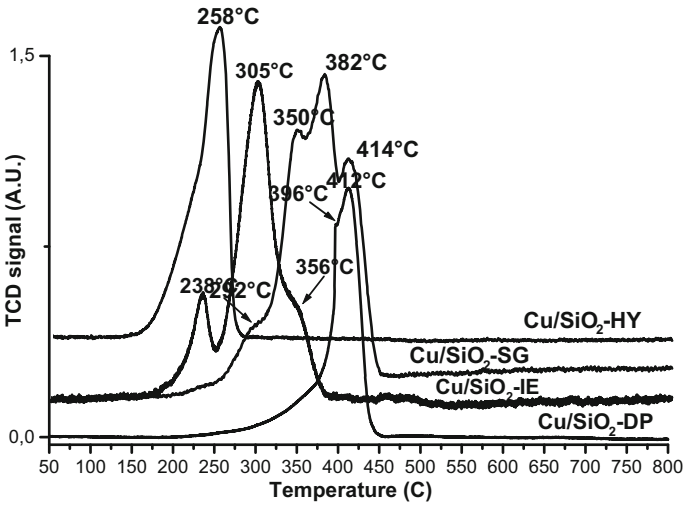

Fig. 4 H_2-TPR profiles of Cu/SiO_2-IE, Cu/SiO_2-DP, Cu/SiO_2-HY, Cu/SiO_2-SG catalysts. Sample mass = 100 mg, from 25 to 850 °C under H_2/Ar flow (5% v/v) with a total flow of H_2 25 mL/min

strongly interact with the support, the isolated Cu^{2+} that weakly interact with the support (the cupric ions have close contact with each other), and small two-dimensional clusters or three-dimensional ones. The second peak observed at higher temperature region is ascribed to the reduction of bulk CuO.

In our case, the XRD results of the samples calcined at 350 °C revealed that no larger CuO particles could be observed (no appeared peaks) but only amorphous or highly dispersed Cu^{2+} species and small clusters that may form. In addition, the TGA study has shown that carbonate and ammonium ions present on "DP" and "HY" catalysts, respectively, resist thermal treatment and they are eliminated above 350 °C, which can make the reduction of copper species more difficult.

For the "DP" catalyst, the TPR profile analysis shows that the peak centered at ca. 396–412 °C is attributed to the reduction of encapsulated CuO species with low surface area silica support or trapped inside the pores because of the presence of carbonate species. The small shoulder observed at 396 °C could account for the two-step reduction ($Cu^{2+} \rightarrow Cu^{+} \rightarrow Cu$). The same behavior could be observed on the "SG" catalyst. In addition to the peak obtained at 414 °C, two other peaks occurring successively at about 350 and 382 °C are related to the presence of two population types of small Cu^{2+} sizes in weakly interaction with support. In the case of Cu/SiO_2-IE, the peak centered at 305 °C with a shoulder at 356 °C, is related to the reduction of isolated Cu^{2+} that weakly interact with the support (the cupric ions have close contact with each other), and small two-dimensional or three-dimensional clusters. The small broad peaks and shoulder observed at a low temperature region (before 300 °C) are assigned to the reduction of isolated highly dispersed Cu^{2+} species.

The total H_2 consumption ratio, reported in Table 1, shows that is superior to 90% in all cases except Cu/SiO_2-HY catalyst, thus suggesting a good accessibility of copper to the reduction step (from Cu^{2+} to Cu^{+} to Cu^{0}). The Cu/SiO_2-HY catalyst shows the lowest total H_2 consumption ratio, suggesting a more difficult reduction, which can be ascribed to a diffusion of copper to the matrix due to the strong metal-support interaction. As shown in Table 1 and Fig. 4, the copper dispersion measured by N_2O titration increases monotonically from 25.5 to 38.4% with the increase of reduction temperature. The catalysts prepared by hydrolysis exhibits low copper dispersion, whereas the catalyst prepared by deposition leads high copper dispersion. As a result, the introduction of a low amount of copper on low specific area silica results in the good metal dispersion. Meanwhile, Cu surface areas exhibit a decreasing trend with the increase of the copper dispersion degree, indicative of the decrease in the surface metallic copper sites. However, the DP sample has the smallest Cu surface area (1.23 $m^2\ g^{-1}$), which is ascribed to the agglomeration of Cu particles or to encapsulated CuO species. To explain catalytic properties, the TPR profiles show that the pre-reduction of catalysts before catalytic reaction up to 250 °C leads mostly to the presence of Cu^{2+} species on low surface area silica support except on the catalysts IE and SG.

SEM images of calcined samples are displayed in Fig. 5. It can be seen that the silica framework is intrinsically different, but well crystallized. The morphology comparison of Cu/SiO_2 catalysts shows that the "SG" and "DP" samples exhibited spherical grains of uniform distribution with diameters lower than1 μm and 3 μm,

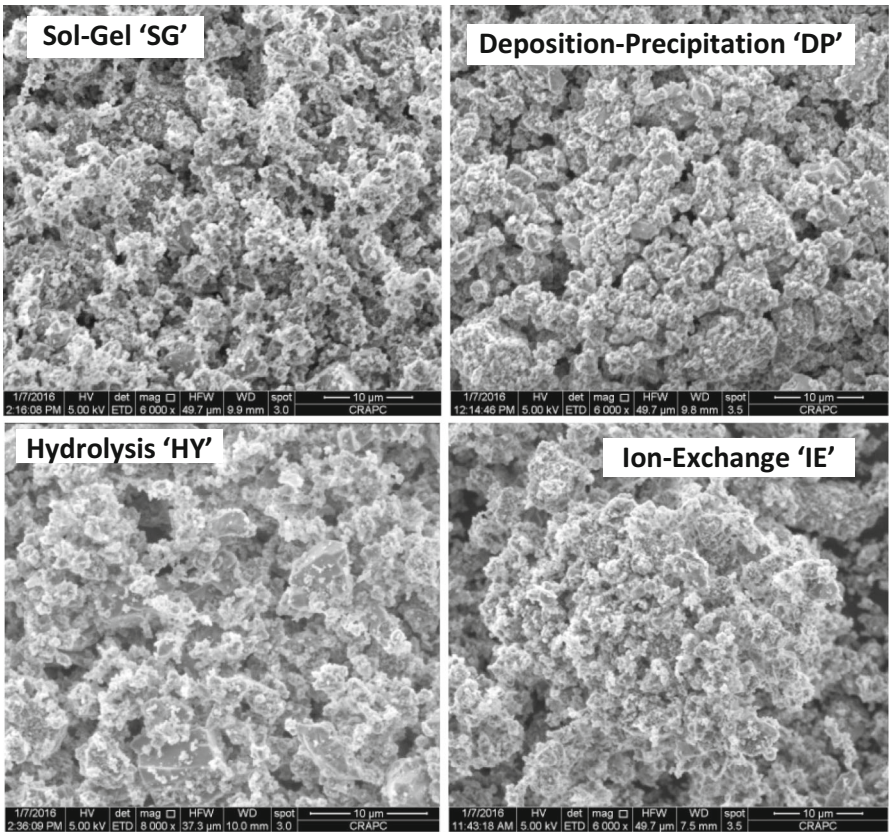

Fig. 5 SEM images of Cu/SiO_2 catalysts prepared per sol–gel (SG), deposition–precipitation (DP), hydrolysis (HY) and ionic exchange (IE)

respectively, whereas more grain aggregation with irregular morphology is noticed in the case of samples prepared by ion exchange and hydrolysis methods.

The UV–Vis spectra of the calcined samples prepared by different methods are shown in Fig. 6. The results indicate that copper incorporated samples exhibit a significant absorption in the visible light region due to the presence of Cu^{2+} species. The spectral analysis shows bands for the catalysts "DP" and "HY" in an interval of 600–800 nm in d-d transitions of Cu^{2+} ions, bands among 400–440 nm, which correspond to the transfer of O–Cu–O and Cu–O–Cu that appears also in "EI" and "DP" catalysts [46].

Catalytic activity

The catalytic behavior of copper-based catalysts supported on low surface area silica prepared by four methods has been examined in the gas phase reduction of benzaldehyde under hydrogen flow at 160 and 200 °C reaction temperature after a pre-reduction step at 250 °C. Figure 7a, b shows the catalytic activities of the

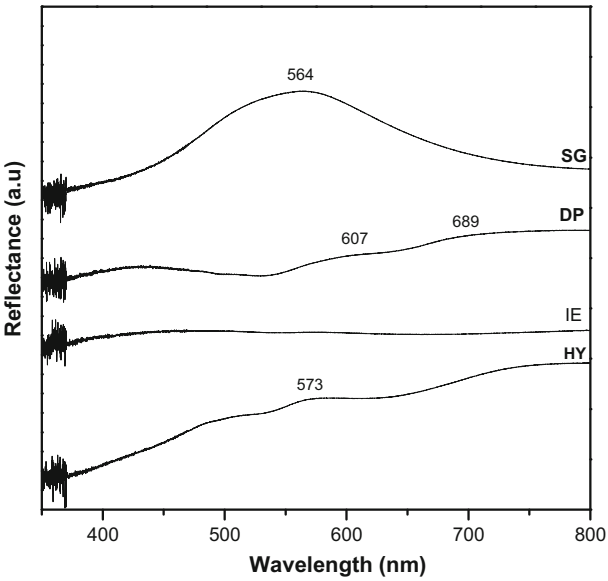

Fig. 6 UV–Vis spectra of Cu/SiO_2-IE, Cu/SiO_2-SG, Cu/SiO_2-HY and Cu/SiO_2-DP catalysts

benzaldehyde reduction with time on stream at reaction temperature 160 and 200 °C, respectively. The low surface area silica used as support is totally inactive, whereas copper-based supported catalysts are active and selective in the gas phase reduction of benzaldehyde, and the reaction products are benzyl alcohol, toluene, and benzene. The activities obtained in the presence of copper prove that the latter is the main component of the active site.

At 160 °C reaction temperature (Fig. 7a), the copper-based catalysts prepared by hydrolysis (HY) and deposition (DP) methods exhibited initial activation before the steady-state is established after 4 h of reaction and the degree of activation depended on the preparation method. It can be noted that Cu/SiO_2 prepared by sol–gel method (SG) is the less active whereas the same catalyst prepared by hydrolysis method (HY) is the most active that exhibits higher activation with time on stream (an increase from 18 to 32 μmol min^{-1} g^{-1}). On Cu/SiO_2-DP catalyst, an increase of activity from 7 to 19 μmol min^{-1} g^{-1} is observed after about 4 h. Conversely, Cu/SiO_2-IE catalyst is the most stable since the beginning of the reaction. At 200 °C reaction temperature, the inverse phenomenon is observed on all catalysts except Cu/SiO_2 prepared by sol–gel method (SG), whose initial activity rate was maintained with time on stream and no deactivation was observed (Fig. 7b). The remainder of the catalysts show initial deactivation before steady-state. On Cu/SiO_2 catalysts prepared by deposition (DP) and hydrolysis (HY), a drop of activity from 49–21 to 53–39 μmol min^{-1} g^{-1}, respectively, is observed after about 4 h working. The decreased activity is the result of poisoning or blocking of active sites by strongly adsorbed oxygen molecules [30].

The steady-state activity rate for all catalysts (Table 2) showed that the level and the order of activity depended on both the preparation method and reaction

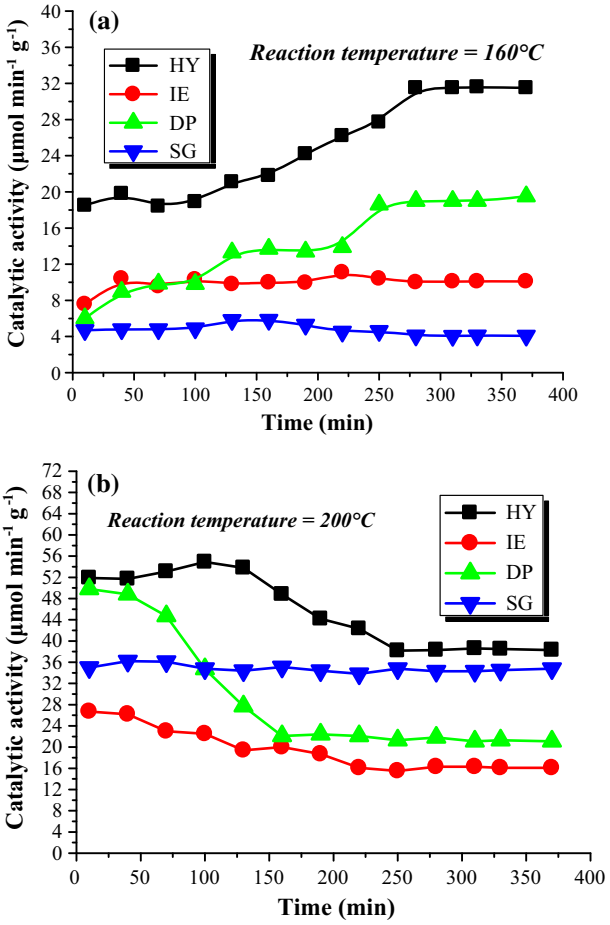

Fig. 7 Catalytic activity per µmol min^{-1} g^{-1} versus time on stream under H_2 flow. Pretreatment conditions: H_2/250 °C. reaction temperatures: **a** 160 °C, **b** 200 °C

temperature. At 160 and 200 °C, the catalyst prepared by hydrolysis is by far the most active, and the catalytic activity order obtained at 200 °C is a follows:

$$Cu/SiO_2\text{-HY} \geq Cu/SiO_2\text{-SG} > Cu/SiO_2\text{-DP} \geq Cu/SiO_2\text{-IE}$$

To correlate the catalytic activity with the characterization results, the decreasing order of activity according to the mode of preparation appears to be related to the pore volume and diameter (see Table 1). Although there is insufficient published data to arrive at any reliable trends regarding pores volume and size effects in –CH=O hydrogenation, we can note the reported decrease in catalytic activity over Cu/SiO_2 prepared by deposition (DP) and ion-exchange (IE) methods (< 0.01 cm^3 g^{-1} and 6 nm) and increase with increasing of pores volume and size over Cu/SiO_2-SG and Cu/SiO_2-HY (> 0.01 cm^3 g^{-1} and 10 nm). The size and volume of the larger pores ensure greater accessibility and dissociation of hydrogen

Table 2 Summary of catalytic activity and selectivity for the gaseous phase hydrogenation over Cu/SiO_2 catalysts

Catalysts	$T_{Reaction}$ (°C)	Activity[a] μmol min^{-1} g^{-1}	Products distribution (% selectivity)[a]		
			Benzyl alcohol	Toluene	Benzene
Cu/SiO_2-DP	160	19	80	5	15
	200	21	45	7	48
Cu/SiO_2-IE	160	10	95	05	–
	200	16	76	24	–
Cu/SiO_2-SG	160	5	97	–	03
	200	35	20	75	05
Cu/SiO_2-HY	160	32	44	50	06
	200	39	–	91	09

[a]Results obtained at steady-state after 4 h of reaction time. Reaction conditions: carrier gas = H_2 and pressure = 1 atm, pre-reduction temperature = 250 °C, reaction temperature = 160 and 200 °C

on the different species of copper formed and its reaction with the reagent. With agreement to the surface structure, the presence of low pore volume and size can lead to decreased adsorption and reaction of carbonyl group with the active sites. The presence of different sizes of copper nano-crystallites interacting with the silica support must lead to a more or less homogeneous distribution of the copper species in the silica support, which makes it difficult to adsorb and dissociate hydrogen [47, 48].

Based on metallic copper surface area and dispersion degree, one important key to high catalytic performance is a large, accessible Cu surface area because larger copper surface area can provide more catalytically active sites for hydrogen dissociation and thus higher conversion. Indeed, the catalyst prepared by hydrolysis with the largest active Cu surface area and smallest dispersion degree exhibits superior catalytic performance to other methods, but favor toluene and benzene as by-products. It can be deduced that the Cu species should be the effective catalytically active centers for dissociating hydrogen in the consecutive hydrogenation of benzaldehyde to toluene. For the rest of the preparation methods, the obtaining of small Cu surface areas is synonymous of the predominance of Cu^{2+} species on the catalysts surface, which leads to a low conversion of benzaldehyde. The higher copper dispersion degree confirms the formation of weak metal-support interactions, making Cu^{2+} reduction more difficult.

On the other hand, the "IE" catalyst with the lowest copper content (2.3 wt%) is the least efficient, whereas the higher copper content obtained on the HY catalyst (3.3 wt%) led to higher activity. In addition and based on TGA results, the presence of heat-resistant carbonate species (Fig. 1) on the "DP" catalyst significantly affects also the catalytic activity. On the contrary, the existence of the copper ammonium complex on the "HY" catalyst conducting to the formation of a single population of readily reducible copper particles (see TPR profiles) could be related to the high activity.

On the basis of the results given in the literature, a strong adsorption of the oxygenated species (as the reagent) on the support surface could cause a blocking of the active sites. Indeed, the adsorption studies of benzaldehyde over several metal oxides confirm the contribution of acid–base properties of few supports such as silica in the reduction of –C=O function. The FTIR study [48] revealed that the adsorption of benzaldehyde on silica involves hydrogen bonding between the oxygen atom of the C=O group and the surface silanol groups, producing surface benzoate species [49, 50].

Selectivity

The gas phase hydrogenation of benzaldehyde is used in an attempt to correlate the benzylacohol selectivity as the main product with the physicochemical properties of the catalysts. As seen in Table 2, over Cu/SiO_2 prepared by several methods, benzaldehyde is converted mainly to benzyl alcohol, toluene and benzene, which are the expected products from successive hydrogenation/hydrogenolysis and decarbonylation, respectively [30, 51]. Under the operating conditions fixed to this reaction, no aromatic ring hydrogenation or its opening was observed. The aromatic ring is unreactive while the –C=O group undergoes a transformation suggesting that benzaldehyde reacts primarily with the catalyst via carbonyl function. In this case, both the aromatic ring and the carbonyl group lie parallel to the active surface [52] and the adsorbed hydrogen preferably attacks the carbonyl group because of the energy barriers [52, 53]. According to the results given in the literature, reaction selectivity is challenging in benzaldehyde hydrogenation due to the number of intermediates and by-products formed, which depends on several parameters such as the nature of metal [6], the nature of phase reaction (liquid or gas) [18, 54], the nature of gas pretreatment and reaction when carried out in gas phase [18], the nature of the solvent when the reaction is carried out in the liquid phase [13].

Whatever the preparation method, benzyl alcohol was obtained over all catalysts at 160 and 200 °C. The observed increasing of benzyl alcohol selectivity with reaction time suggests that it is mostly formed as the primary product of direct hydrogenation of benzaldehyde (Fig. 8). Between 160 and 200 °C, the results summarized in Table 2 reveal that the high benzyl alcohol selectivity appeared on the least active catalysts prepared by deposition (80% at 160 °C), sol–gel (97% et 160 °C) and ion-exchange methods (95% at 160 °C), whereas the high activities encouraged the apparition of toluene as the principal product with high selectivity particularly at 200 °C on Cu/SiO_2 catalysts prepared by sol–gel and hydrolysis methods. For all catalysts, when the reaction temperature increases, the benzyl alcohol selectivity decreases and benzaldehyde conversion increases. From the characterization of catalysts, we can conclude that the differences of selectivity and conversion would not be related to the specific surface area since all catalysts have the similar surface data. The state and distribution of copper species in the catalysts may be the key factors to the reaction.

Several pertinent studies have examined the importance of the different oxidation states of copper in the hydrogenation reactions, but without a general agreement on the copper oxidation state at the origin of benzyl alcohol formation from benzaldehyde.

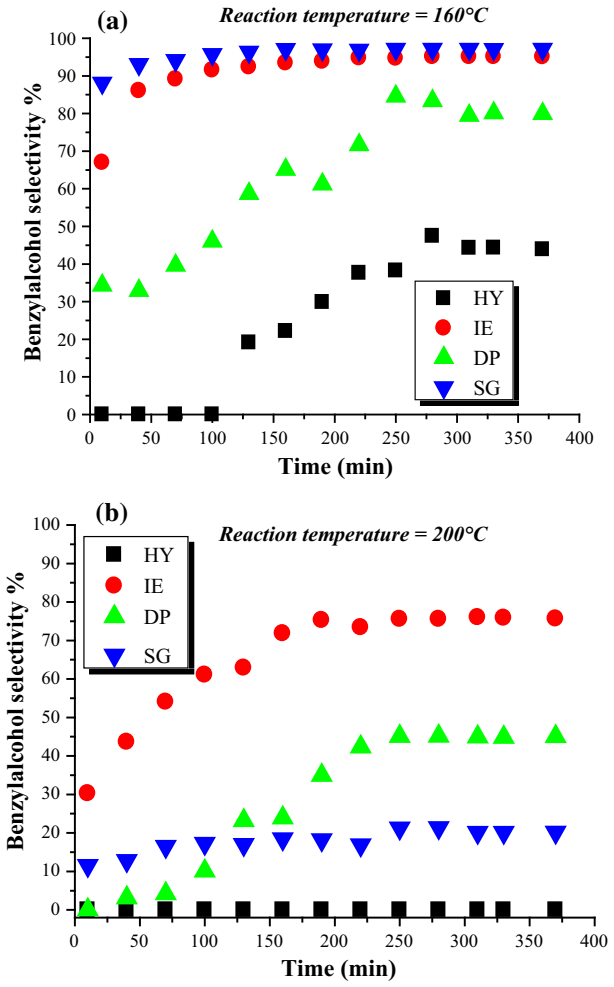

Fig. 8 Benzyl alcohol selectivity versus time on stream under H_2 flow, pressure = 1 atm, reaction temperatures: **a** 160 °C, **b** 200 °C

Before the reduction temperature 250 °C and in agreement with N_2O titration results, the TPR analysis (Fig. 4) shows that no Cu^+ or Cu^0 species are detected in all catalysts except on "Cu/SiO_2-HY" and "Cu/SiO2-IE" (a small amount is reduced). For the rest of the catalysts the predominant species are mainly the isolated Cu^{2+} that weakly interacts with the support and small copper clusters. On the catalyst prepared by hydrolysis method, the reduction of a good amount of Cu^{2+} species in strong interaction with the support could be at the origin of the low benzyl alcohol selectivity.

The formation of benzyl alcohol as a primary product from benzaldehyde hydrogenation occurs via a nucleophilic mechanism where the carbonyl group is adsorbed and activated at the metal/support interface [30]. A co-planar form of benzaldehyde adsorption to the catalyst surface facilitates C=O polarization, making the oxygen sensitive to nucleophilic attack with proton transfer to generate benzyl

alcohol [21]. The possible reaction pathways proposed for hydrogenation of benzaldehyde are shown in Fig. 9.

At the same time, high selectivity of toluene is obtained with "HY" catalyst. So it is easy to conclude that the ability of hydrogenation/hydrogenolysis is related to the CuO species reduced to Cu^0 during pretreatment and reaction, which is the main reactive site for toluene formation. The results suggest that the highly dispersed Cu^{2+} ions were the active phase for the obtaining of highly toluene selectivity, whereas the weakly dispersed Cu^{2+} species were the active site for the benzyl alcohol formation. The obtained toluene as product from successive reaction hydrogenation of benzaldehyde or benzyl alcohol may be favored by a strong interaction between oxygen of carbonyl or alcohol functions and the surface with

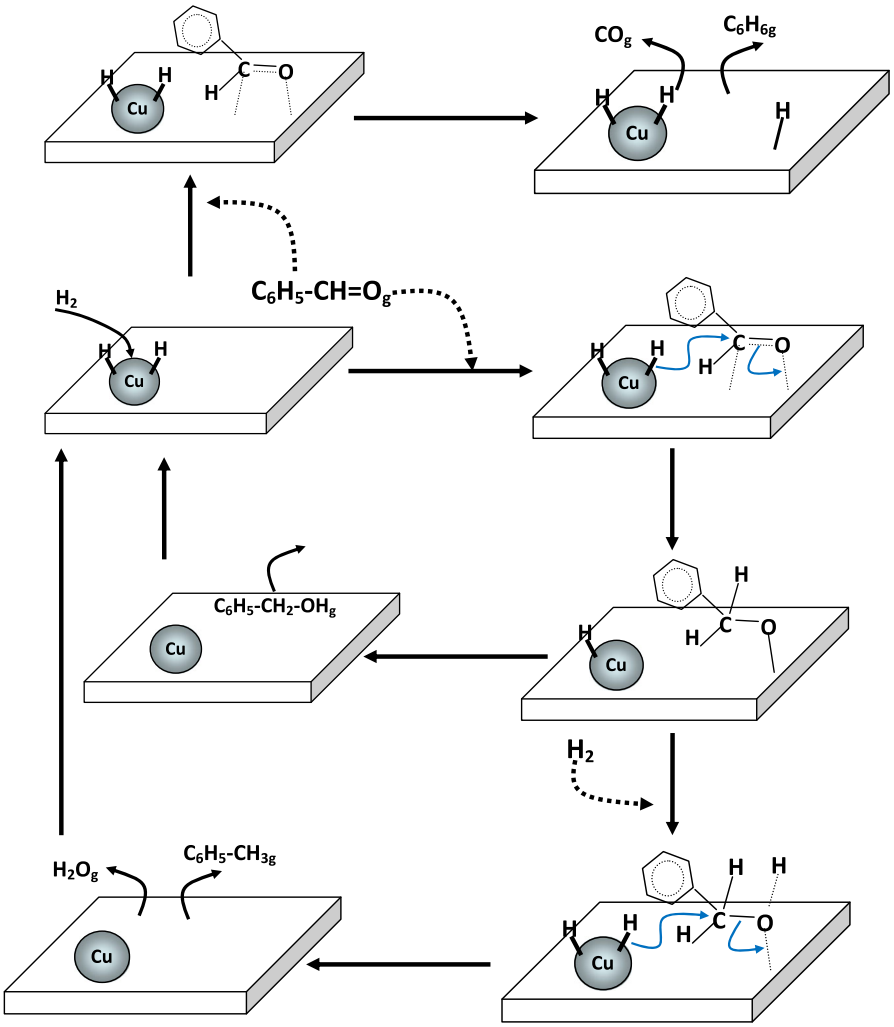

Fig. 9 Proposed mechanism for benzaldehyde hydrogenation over Cu/SiO_2 catalysts

hydrogenolytic cleavage of C=O or C–OH by dissociated hydrogen. The toluene production from benzaldehydde could be the most probable pathway because of the electrophilic character of C=O which renders this functionality more reactive relative to O–H [13]. Keane et al. [6] showed that the rate of toluene production over Ni/Al_2O_3 from benzaldehyde was significantly higher than that obtained from benzyl alcohol and this pathway can be taken to be the predominant route to toluene.

In contrast to the other preparation methods, the most selective catalyst to benzyl alcohol (Cu/SiO_2-IE) does not form any benzene as a by-product. This remarkable difference suggests that the formation of benzene requires an important hydrogenation/hydrogenolysis activity. Indeed, benzene selectivity obtained on the "DP" catalyst (15–48%), suggests the participation of copper species, which are difficult to reduce (from 350 to 450 °C in the TPR profile). This phenomenon is probably attributed to isolated Cu(II) enveloped within the SiO_2 matrix and formed small clusters, which might find access difficult or reduced by hydrogen or reagent molecules.

Conclusion

Cu/SiO_2 catalysts have been successfully synthesized by several methods and the surface structure of the catalysts is determined by the preparation method. High selectivity to benzyl alcohol and low conversion of benzaldehyde were observed on the "IE" catalyst, whereas high selectivity to toluene and high benzaldehyde conversion were observed on the "HY" sample. The hydrogenation activities of all catalysts were strongly dependent on their surface structures. Based on the textural and structural results, the different distribution of Cu^{2+} species over all catalysts have been observed. Readily reducible copper species that may be reduced to metallic copper are responsible for the formation of toluene, while Cu^{2+} species which reduce only at higher temperatures lead to the formation of benzyl alcohol and benzene. The small CuO clusters that may not be reduced to metallic copper are the active sites to catalyze the benzaldehyde hydrogenation reaction and to give benzyl alcohol as the primary product. The results presented in this work provided insight into the relationship between the surface structures of the catalysts determined by the preparation methods and the catalytic behaviors that were accordingly affected.

Compliance with ethical standards

Conflict of interest All authors declare that they have no conflict of interest.

References

1. B. Nair, Int. J. Toxicol. **20**, 23 (2001)
2. R.K. Marella, C.K.P. Neeli, S.R.R. Kamaraju, D.R. Burri, Catal. Sci. Technol. **2**, 1833 (2012)
3. G.D. Yadav, P.H. Mehta, Catal. Lett. **21**, 391 (1993)
4. C.C. Guo, Q. Liu, X.T. Wang, H.Y. Hu, Appl. Catal. A Gen. **282**, 55 (2005)
5. J.A. Schreifels, P.C. Maybury, W.E. Swartz, J. Org. Chem. **46**, 1263 (1981)

6. N. Perret, F. Cardenas-Lizana, M.A. Keane, Catal. Commun. **16**, 159 (2011)
7. W. Liu, Y. Li, X. Chen, P. Zhang, P. Yi, Y. Zhou, Z. Huang, Asian J. Chem. **25**, 1565 (2013)
8. D. Divakar, D. Manikandam, G. Kalidoss, Catal. Lett. **125**, 277 (2008)
9. D.C. Higgins, D. Meza, Z.W. Chen, J. Phys. Chem. C **114**, 21982 (2010)
10. S. Abate, R. Arrigo, M.E. Schuster, S. Perathoner, G. Centi, A. Villa, D. Sub, R. Schlögl, Catal. Today **157**, 280 (2010)
11. M. Li, X. Wang, F. Cardenas-lizana, M.A. Keane, Catal. Today **279**, 19 (2017)
12. A. Aboulayt, A. Chamellan, M. Marzin, J. Saussey, F. Maugé, J.C. Lavalley, C. Mercier, R. Jacquot, Stud. Surf. Sci. Catal. **78**, 131 (1993)
13. M.A. Vannice, D. Poondi, J. Catal. **169**, 166 (1997)
14. A. Saadi, M.M. Bettahar, Z. Rassoul, Stud. Surf. Sci. Catal. **130**, 2261 (2000)
15. J.T. Bhanushali, I. Kainthla, R.S. Keri, B.M. Nagaraja, Chem. Sel. **1**, 3839 (2016)
16. M.L. Barbelli, G.F. Santori, N.N. Nichio, Bioresour. Technol. **111**, 500 (2012)
17. Z. Wu, Y. Mao, M. Song, X. Yin, M. Zhang, Catal. Commun. **32**, 52 (2013)
18. D. Haffad, U. Kameswari, M.M. Bettahar, A. Chambellan, J.C. Lavalley, J. Catal. **172**, 85 (1997)
19. M.A. Vannice, D. Poondi, J. Catal. **178**, 386 (1998)
20. F. Coloma, A. Sepuldeva-Escribano, J.L.G. Fierro, F. Rodriguez-Reinoso, Appl. Catal. A Gen. **148**, 63 (1996)
21. K. Lanasri, A. Saadi, K. Bachari, D. Halliche, O. Cherifi, Stud. Surf. Sci. Catal. **174**, 1279 (2008)
22. R.M. Mironenko, O.B. Belskaya, T.I. Gulyaeva, M.V. Trenikhin, A.I. Nizovskii, A.V. Kalinkin, V.I. Bukhtiyarov, A.V. Lavrenov, V.A. Likholobov, Catal. Today **279**, 2 (2017)
23. D. Procházková, P. Zámostný, M. Bejblová, L. Červený, J. Čejka, Appl. Catal. A: Gen. **332**(1), 56 (2007)
24. T. Turek, D.L. Trimm, N.W. Cant, Catal. Rev. Sci. Eng. **36**, 645 (1994)
25. B. Hu, Y. Yamaguchi, K. Fujimoto, Catal. Commun. **10**, 1620 (2009)
26. R.D. Cortright, M. Sanchez-Castillo, J.A. Dumesic, Appl. Catal. B: Environ. **39**, 353 (2002)
27. M.A. Natal-Santiago, M.A. Sánchez-Castillo, R.D. Cortright, J.A. Dumesic, J. Catal. **193**, 16 (2000)
28. A.M. Hengne, C.V. Rode, Green Chem. **14**, 1064 (2012)
29. M. Dixit, M. Mishra, P.A. Joshi, D.O. Shah, Procedia Eng. **51**, 467 (2013)
30. A. Saadi, Z. Rassoul, M.M. Bettahar, J. Mol. Catal. A: Chem. **164**, 205 (2000)
31. L.A.M. Hermans, J.W. Geus, Stud. Surf. Sci. Catal. **3**, 113 (1979)
32. S. Lambert, C. Cellier, P. Grange, J.P. Pirard, B. Heinrichs, J. Catal. **221**, 335 (2004)
33. P. Munnik, P.E. de Jongh, K.P. de Jong, Chem. Rev. **115**(14), 6687 (2015)
34. A. Miyazaki, I. Balint, K.I. Aika, Y. Nakano, J. Catal. **204**(2), 364 (2001)
35. D.G. Mustard, C.H. Bartholomew, J. Catal. **67**(1), 186 (1981)
36. A.G. Boudjahem, S. Monteverdi, M. Mercy, M.M. Bettahar, J. Catal. **221**, 325 (2004)
37. P. Barrett, E.G. Joyner, P.P. Halenda, J. Am. Chem. Soc. **73**, 373 (1951)
38. Y. Cheng, X. Niu, T. Zhao, F. Yuan, Y. Zhu, H. Fu, J. Inorg. Chem. **28**, 4988 (2013)
39. O. Lezla, E. Bordes-Richard, P. Courtine, G. Hequet, J. Catal. **170**, 346 (1997)
40. J.D. Ortego, S. Jackson, G.S. Yu, H. McWhinney, D.L. Cocke, J. Env. Sci. Heal. A **24**(6), 589 (1989)
41. S. Xiao, Y. Zhang, P. Gao, L. Zhong, X. Li, Z. Zhang, Y. Sun, Catal. Today **281**, 327 (2017)
42. A. Tirsoaga, B. Cojocaru, C. Teodorescu, F. Vasiliu, M.N. Grecu, D. Ghica, V.I. Parvulescu, H. Garcia, J. Catal. **341**, 205 (2016)
43. Z. Wang, Q. Liu, J. Yu, T. Wu, G. Wang, Appl. Catal. A Gen. **239**, 87 (2003)
44. W.P. Dow, Y.P. Wang, T.J. Huang, J. Catal. **160**, 155 (1996)
45. W.P. Dow, Y.P. Wang, T.J. Huang, Appl. Catal. A Gen. **190**, 25 (2000)
46. A.N. Pestryakov, V.P. Petranovskii, A. Kryazhov, O. Ozhereliev, N. Pfänder, A. Knop-Gericke, Chem. Phys. Lett. **385**(3), 173 (2004)
47. C.A. Koutstaal, P.A.J.M. Angevvare, V. Ponec, J. Catal. **143**, 573 (1993)
48. J. March, *Advanced Organic Chemistry International, Stud Ed* (McGraw-Hill, Tokyo, 1977)
49. N. Tahir, Z. Abdelssadek, D. Halliche, A. Saadi, R. Chebout, O. Cherifi, K. Bachari, Stud. Surf. Sci. Catal. **174**, 1287 (2008)
50. T.F. Mao, J.L. Falconer, J. Catal. **123**, 443 (1990)
51. A. Ausavasukhi, T. Sooknoi, D.E. Resasco, J. Catal. **268**, 68 (2009)
52. D. Poondi, M.A. Vannice, J. Mol. Catal. A: Chem. **124**, 79 (1997)
53. A. Saadi, Z. Rassoul, M.M. Bettahar, J. Mol. Catal. A: Chem. **258**, 59 (2006)
54. L. Červený, Z. Bělohlav, M.N.H. Hamed, Res. Chem. Intern. **22**, 15 (1996)